Recovering the 3D Shape and Respiratory Motion of the Rib using Chest X-Ray Image

Myint Myint Sein[*1], Mitsuru Komizu[*2], Yoshio Yanagihara[*3] and Hiromitsu Hama[*3]

Abstract -This aper presents a new method for the reconstruction of the 3D shape and respiratory motion of the rib from the 2D X-ray images. Each rib has been represented as a curve and its control points are estimated by the cubic B-spline curve iteration algorithm. To recover the 3D motion and the control points of the ribs using the 2D control points, the factor decomposition algorithm for projective structure and motion has been developed. The measurement matrix has been built with the corresponding control points of each curve. By means of the control points, instead of all points of a curve, data capacity and computational times are reduced. Furthermore, the precision of matching pairs of a rib in multiple images is improved. The estimation errors are not appeared only due to the 2D control point approximation but also the computation of the 3D control points. The experiment with X-ray images has been performed and the effectiveness of the proposed technique has been confirmed through the results with acceptable errors. This approach can be applied to examine the chest expansion for inspecting the pulmonary diseases.

Key words: Respiratory motion of the rib, B-spline curve control points, measurement matrix, singular value decomposition, thorax, chest X-ray images

1.   Introduction

Analysis of chest wall motion is an important research field in the respiratory physiology. Recently, the studies of the respiratory movement in the 3D configuration of the chest wall have been paid substantial attention by researchers. The chest or breast shape and   position will be changed through the rib motion on the occasion of the breathing relative to the contraction of the breathing muscle. In many research works CT images produced by the high resolution and fast CT scanners are mainly used to detect the chest wall movement. There are some related approaches[1-7] to generate and recover the motion of the chest wall and ribs. Cala et al.[1] applied four TV cameras to detect the 86 hemispherical reflective markers arranged circumferentially on the chest wall. Groote et al.[2] also used an automatic motion analyzer, the ELITE system, to investigate the chest wall motion during tidal breathing. Two TV cameras are used in their system to record the 36 markers. Jordanoglou[3] recovered the motion vector of a rib. According to this, the rib rotates around only one axis and its shape doesn't change during breathing. The spatial vectors at several points along a rib are parallel to one another and they have a constant direction on successive breathing cycles. Park   et al.[5] analyzed the 3D rib motion for CT images.

In this paper a new method to recover the shape and respiratory motion of the ribs is proposed. Each rib is consid-

ered as a curve and its 3D shape and motion are recovered from the 2D X-ray images. The control points of each curve are estimated by the cubic B-spline curve approximation algorithm. In this algorithm the iteration method based on the learning algorithm[8,9] is employed for minimizing the approximation errors. A curve which well resembles the original curve can be reconstructed from these control points. Then, the corresponding pairs of control points of each curve are investigated through the images. The measurement matrix has been built by gathering the corresponding control points of each curve of the X-ray image frames. The shape and motion of a single object can be recovered from the image stream under orthography[7]. In our previous work[9] the 3D shape of the object has been reconstructed by the singular value decomposition approach. In this work we compute not only the 3D control points but also the motion of each rib. The 3D curve has been reformed by these control points. Average motion parameter of the rib is approximated from the motion of each curve. Moreover, 3D motion and the set of control points of all curves can be computed from the set of corresponding control points of all curves in successive image frames. It is possible to inspect some pulmonary diseases from the chest expansion observed by this approach.

This paper is organized as follows. The structure of thorax and the B-spline control points   approximation algorithm are introduced in Section 2. The detail of the proposed method based on the factorization algorithm is discussed in Section 3. The experiment and results are described in Section 4. Finally, the conclusions and discussion are presented in Section 5.

2. Rib and B-spline control points

1)   Structure of the thorax

In this Section the structure of the thorax will be considered. Figure 1 illustrates the model of thorax which is formed by the twelve pairs of left - right ribs connected with the spine (backbone). Figure 2 shows an example of an X-ray image of a male subject. The position of each rib will change due to the breathing. Figure 3 presents the movement of
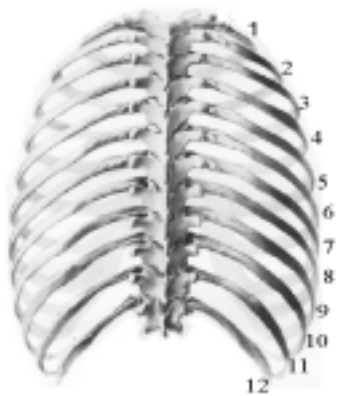

Fig. 1 Model of thorax (back).
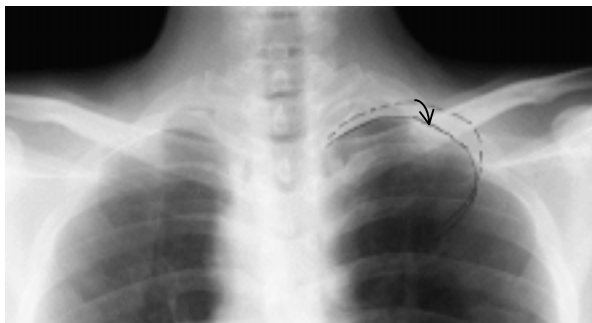

Fig. 2 An X-ray image.

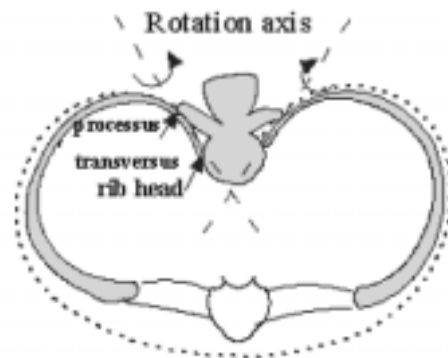**Fig. 3** The movement of a rib between two images.

Fig. 4 Rotation axis of rib.

rib 2 between two images. Each rib touches the backbone in two places, which are the rib head (caput costae) and process transverses, and each rib rotates centering on the axis which passes these places [5]. Then, the rotational axes of left- right rib are illustrated by the cross section of thorax in figure 4.

2) Process

The general process of our method for recovering the shape and motion of the rib is shown in figure 5. The X-ray images are obtained by an X-ray radiology device during breathing.

3) Control points of a rib

Each rib can be represented as a curve. A set of control points needs to estimate for representing the feature of the curve. B-spline control points estimation algorithm is used in this work. A B-spline curve $P(t)$ of degree n can be defined in terms of the set of control points Q_i $(i = 0,1,..,\ n)$ with the parameter $t\ (0 \leq t \leq 1)$,

$$P(t) = \sum_{i=0}^{n} B_{in}(t) Q_i \ , \tag{1}$$

where $B_{in}(t)$ is called Bernstein polynomial. By assuming n=3, the cubic B-spline curve $P(t)$ can be reduced into a matrix form from Eq. (1) as:

$$P(t) = \begin{bmatrix} B_0(t) & B_1(t) & B_2(t) & B_3(t) \end{bmatrix} Q , \tag{2}$$

where $Q = \begin{bmatrix} Q_0 & Q_1 & Q_2 & Q_3 \end{bmatrix}^T$, $B_0(t) = \frac{1}{6}(1-t)^3$, $B_1(t) = \frac{1}{2}t^3 + \ t^2 + \frac{2}{3}$, $B_2(t) = \frac{1}{2}t^3 + \frac{1}{2}t^2 + \frac{1}{2}t + \frac{1}{6}$,

$B_3(t) = \frac{1}{6}t^3$ $\quad (0 \leq t \leq 1)$. $B_0(t)$, $\quad B_1(t)$, $B_2(t)$ and $B_3(t)$ vary with the parameter $t\ (0\ \leq\ t\ \leq\ 1)$.

In case when $\quad t = 0$, the point P_i of the cubic B-spline curve can be deduced from Eq. (2).

$$P_i = \frac{1}{6}Q_{i-1} + \frac{2}{3}Q_i + \frac{1}{6}Q_{i+1} \ \ (i = 1,..,m-1), \tag{3}$$

where m is the number of computed control points of the initial control points i on the curve. For instance, the B-spline control points for a free curve are shown in figure 6. To examine the control points Q_i concerning with the
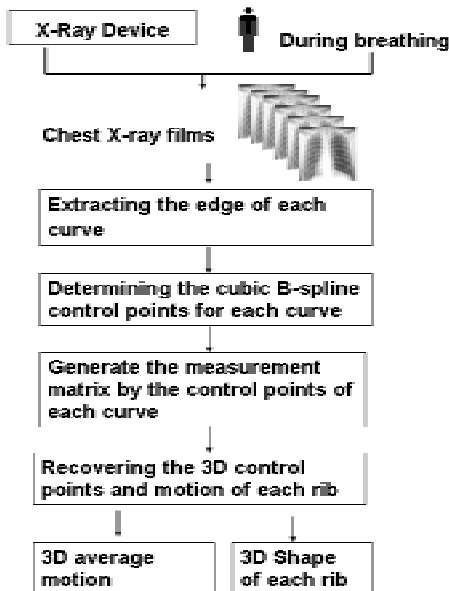

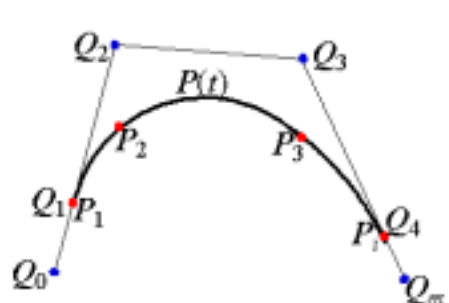
Fig. 5 The scheme of the proposed method.

Fig. 6 B-spline control points for a curve.

assumed points $\boldsymbol{P}_i$ on a free curve, first the location of the points $\boldsymbol{P}_i$ on the curve must be estimated. It is clear that the first and last control points of the curve are the end points of the curve.

The second and third control points of the B-spline curve are assumed to be located at the tangent lines made by the end points of the curve. The locations of point $\boldsymbol{P}_2$ and $\boldsymbol{P}_3$ are assumed by the location of the $(\frac{N}{5})$th and $(N-\frac{N}{5})$th points of the curve by the learning algorithm[8]. Here, N is the total number of points in the curve. At the k-th iteration of learning the control point $\boldsymbol{Q}_i$ $(i=1,..,m-1)$ is,

$$\boldsymbol{Q}_i^k = \frac{3}{2}\boldsymbol{P}_i - \frac{1}{2}(\boldsymbol{Q}_{i-1}^{k-1} + \boldsymbol{Q}_{i+1}^{k-1}) \cdot \tag{4}$$

To obtain the accurate control points of a curve, the difference δ_i of the control points $\boldsymbol{Q}_i$ from $(k-1)$th to k-th iteration is computed, i.e.,

$$\delta_i = \boldsymbol{Q}_i^k - \boldsymbol{Q}_i^{k-1}. \tag{5}$$

For any open curve, the set of $\boldsymbol{Q}_j (j=0,..,m)$ which contains $\boldsymbol{Q}_i$ $(i=1,..,m-1)$, $\boldsymbol{Q}_0 = \boldsymbol{Q}_1$ and $\boldsymbol{Q}_m = \boldsymbol{Q}_{m-1}$ is said to be the set of robust B-spline control points when δ_i is sufficiently small, i.e., $max\,|\delta_i| \le \varepsilon$. Let us suppose the value of the minimum permissible error ε be equal to 0.00001 in this work. We decided this value empirically. If $max\,|\delta_i| > \varepsilon$, $\boldsymbol{Q}_j$ is replaced as $\boldsymbol{Q}_i = \delta_i + \boldsymbol{Q}_i$, $\boldsymbol{Q}_0 = \boldsymbol{Q}_1$ and $\boldsymbol{Q}_m = \boldsymbol{Q}_{m-1}$ and examine again for the different δ_i from the $(k-1)$th to the k-th iteration. If the error is not small enough then the new control points are assumed to be near the old one.

3.   Recovering the 3D rib motion and control points based on the factor decomposition

In this Section, 3D B-spline control points of each rib are computed from the 2D curve of the thorax by the factorization approach. Thorax contains twelve pairs of left-right ribs. The B-spline control points of each rib are estimated from the 2D X-ray images acquired during breathing. The $2m \times n$ measurement matrix $\boldsymbol{B}_i$ $(i=1,2,...,k)$ is generated by tracking the control points of the k-th B-spline curve through the successive images. Let us consider the measurement matrix under the full perspective projection model. Then $\boldsymbol{B}_i$ can be expressed in matrix form:

$$\boldsymbol{B}_i = \begin{bmatrix} \boldsymbol{X} \\ \boldsymbol{Y} \end{bmatrix} \quad (i=1,2,...,k) \tag{6}$$

where $\boldsymbol{X}$ and $\boldsymbol{Y}$ are the x and y component of the control points, respectively.

The registered measurement matrix $\widetilde{\boldsymbol{B}}$ is derived from the matrix $\boldsymbol{B}_i$ relative to the object center coordinate system and factorized into three matrices as follows:

$$\widetilde{\boldsymbol{B}} = \boldsymbol{U}\boldsymbol{\Sigma}\boldsymbol{V}^T, \tag{7}$$

where the eigen vectors of $\widetilde{\boldsymbol{B}}\widetilde{\boldsymbol{B}}^T$ and $\widetilde{\boldsymbol{B}}^T\widetilde{\boldsymbol{B}}$ are the columns of $\boldsymbol{U}$ and $\boldsymbol{V}$, and they satisfy

$$\boldsymbol{U}^T\boldsymbol{U} = \boldsymbol{V}^T\boldsymbol{V} = \boldsymbol{V}\boldsymbol{V}^T = \boldsymbol{I}, \tag{8}$$

where $\boldsymbol{\Sigma}$ is a diagonal matrix of positive decreasing singular values and the number of nonzero singular values is related to the rank of $\widetilde{\boldsymbol{B}}$, and $\boldsymbol{I}$ is the unit matrix. Due to the noisy and unmatched point measurements, $\widetilde{\boldsymbol{B}}$ will be at most rank 4 in real situations. And the diagonal matrix $\boldsymbol{\Sigma}$ will also contain more than 4 nonzero singular values. Therefore, we pay attention only the first four columns of $\boldsymbol{U}$ and the first four rows of $\boldsymbol{V}^T$, and denote them $\widetilde{\boldsymbol{U}}$ and $\widetilde{\boldsymbol{V}}^T$, respectively. $\widetilde{\boldsymbol{\Sigma}}$ is also created by the first four diagonal elements of $\boldsymbol{\Sigma}$. This consideration is made for

single object. $\widetilde{U}$, $\boldsymbol{\Sigma}$ and $\widetilde{V}^{T}$ are also changed relating to the rank.

The registered measurement matrix $\widetilde{B}$ can be expressed as follows

$$\widetilde{B} = RS \quad , \tag{9}$$

where R represents the camera rotation and S represents the 3D position of the object with respect to the object center. For the best possible approximation, Eq. (7) can be reduced as

$$\hat{B} = \widetilde{U}\widetilde{\Sigma}\widetilde{V}^{T} \; . \tag{10}$$

Let us define

$$\hat{R} = \widetilde{U}\,(\widetilde{\Sigma})^{1/2} \quad , \tag{11}$$

$$\hat{S} = (\widetilde{\Sigma})^{1/2} V^{T} . $$

Then we can rewrite Eq. (10) as

$$\hat{B} = \hat{R}\,\hat{S} \quad , \tag{12}$$

where $\hat{R}$ and $\hat{S}$ are the linear transformation of the rotation and shape matrices R and S, respectively. The rotation and shape are computed by using any invertible 4×4 matrix A,

$$R = \hat{R}A \; , \tag{13}$$

$$S = (A)^{-1}\hat{S} \; . \tag{14}$$

To obtain the exact solution, A is defined as concatenation of two blocks,

$$A = \left[A_{\Omega} \mid A_{t}\right]. \tag{15}$$

The 4×3 matrix A_{Ω} is related to the rotational component and the 4×1 matrix A_{t} is related to translation. The matrix A_{Ω} is constrained by the orthonormality of axis vectors i_{F}^{T} and j_{F}^{T}. We have the system of equations:

$$\begin{aligned}
\hat{i}_{m} A_{\Omega} A_{\Omega}^{\;T} \hat{i}_{m}^{T} &= 1, \\
\hat{j}_{m} A_{\Omega} A_{\Omega}^{\;T} \hat{j}_{m}^{T} &= 1, \\
\hat{i}_{m} A_{\Omega} A_{\Omega}^{\;T} \hat{j}_{m}^{T} &= 0.
\end{aligned} \tag{16}$$

The matrix A_{Ω} can be obtained from the above system of equations. To determine the matrix A_{t}, the centroid of the set of control points has been considered as,

$$\overline{B} = \begin{bmatrix} \dfrac{1}{N}\sum X \\ \dfrac{1}{N}\sum Y \end{bmatrix} = R\overline{S} = [\hat{R}A_{\Omega} \mid \hat{R}A_{t}]\begin{bmatrix} \overline{P} \\ 1 \end{bmatrix} \; , \tag{17}$$

where $\overline{P} = \dfrac{1}{N}(\sum P_{i}) = 0$ is the centroid of the object. It follows from Eq. (17) that

$$\overline{B} = \hat{R}A_{t} \quad , \tag{18}$$

and the matrix A_{t} is,

$$A_{t} = (\hat{R}^{T}\hat{R})^{-1}\hat{R}^{T}\overline{B} \; . \tag{19}$$

Once the matrix A has been found, the rotation and structure of each curve are recovered from Eq. (13), Eq. (14) and Eq. (19). The rotation matrix R contains motion Ω and translation T as

$$R = \left[\begin{array}{c:c} \Omega & T \\ \hdashline 0 & 1 \end{array}\right] , \tag{20}$$

where $\quad \Omega = \begin{bmatrix} r_{11} & r_{12} & r_{13} \\ r_{21} & r_{22} & r_{23} \\ r_{31} & r_{32} & r_{33} \end{bmatrix}$

and $\quad T = \begin{bmatrix} t_1 & t_2 & t_3 \end{bmatrix}^T$.

The motion of the rib can be described by the rotation angle and direction concerning with the rotation axis. Three characteristic values can be reduced from Ω by the eigen value decomposition. One value will be a real value and others two are complex. The eigen vector relating to the unit value is represented for the direction of the rotation axis. And the rotation angle is computed from two complex values.

4. Experiments and results

The chest X-ray images are obtained from the healthy male subjects by the radiology device during respiration. Table 1 summarizes the current performance. The center pixel of the image is (256,256). The distance between a film plate and the radiology device is fixed to 100 cm. The camera model can be considered as a weak-perspective model by the ratio of the object depth and distance from the X-ray device. A PC with Pentium III 750 MHz processor and 768 MB memory is used in this experiment. Matlab version 6.1 which is the high performance numeric computation and visualization software is employed to analyze the data. Some processing steps of curve extraction have been performed with Adobe Photoshop 6.0J. Rib regions are extracted from the X-ray image by processing the images. Due to the nature of the rib, the smooth shape of curve can't be obtained from the centerline and upper edge line of the rib.

Rib 1 is difficult to extract separately and rib 10, rib 11 and rib 12 can't be seen clearly in some images. So the ribs 2 to 9 are only considered to extract the lower parts of their edges. The simulation of the B-spline control point estimation for a curve has been done. The simulation results are shown in figure 7. For each curve of ribs, the set of control points including four control points is examined by the cubic B-spline control points finding algorithm. A B-spline curve and its control points for rib 2 are shown in figure 8. The accuracy of the control point approximation for the ribs is shown in figure 9. The average errors for the curve detection by B-spline control points are shown in **Table 2**. And the 3D motion and B-spline control points for each curve are computed based on the singular value

Table 1. Performance of the subjects and X-Ray device

Number of subjects	10
Average age	42
Frame rate	Up to 9 frames during 0.3sec
Average depth of the body	17 cm
Distance between a film plate and the radiology device	100 cm

(a)   (b)
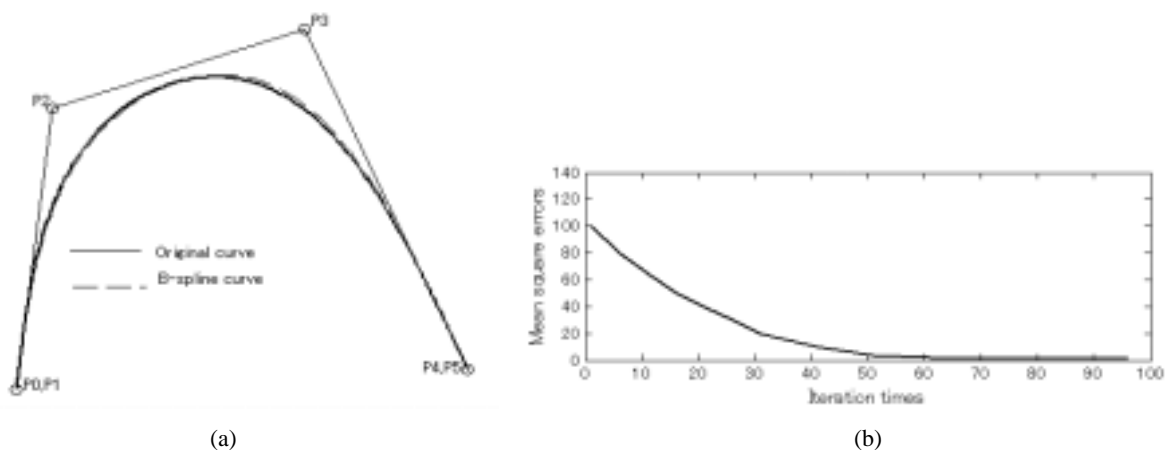
Fig 7 Simulation results:(a)Original curve and B-spline curve with control points, (b)Errors concerning with the iteration times.

decomposition method. The 3D recovered shapes of rib2, rib 3, rib4, rib 5, rib 6 and rib 9 are shown in **Fig. 10**. The average computation times for recovering the 3D motion and the drawing of B-spline curve for each curve are 0.2 sec. The max-rotation angle of the ribs for each subject (S) and average motion angles of the ribs are illustrated in **Fig. 11**(a) and 11(b), respectively. The effectiveness of our proposed method was confirmed from the experimental results.
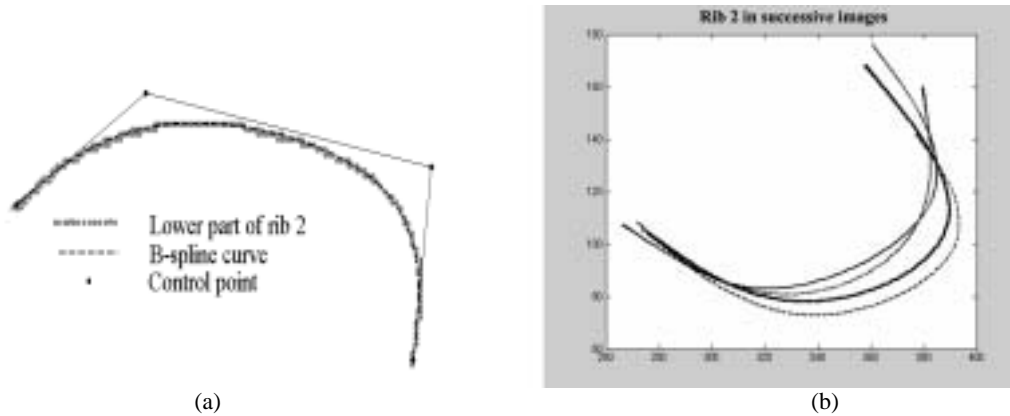

(a)   (b)

Fig. 8 B-spline curves and control points for rib 2:(a) Original curve and reconstructed curve of rib 2,

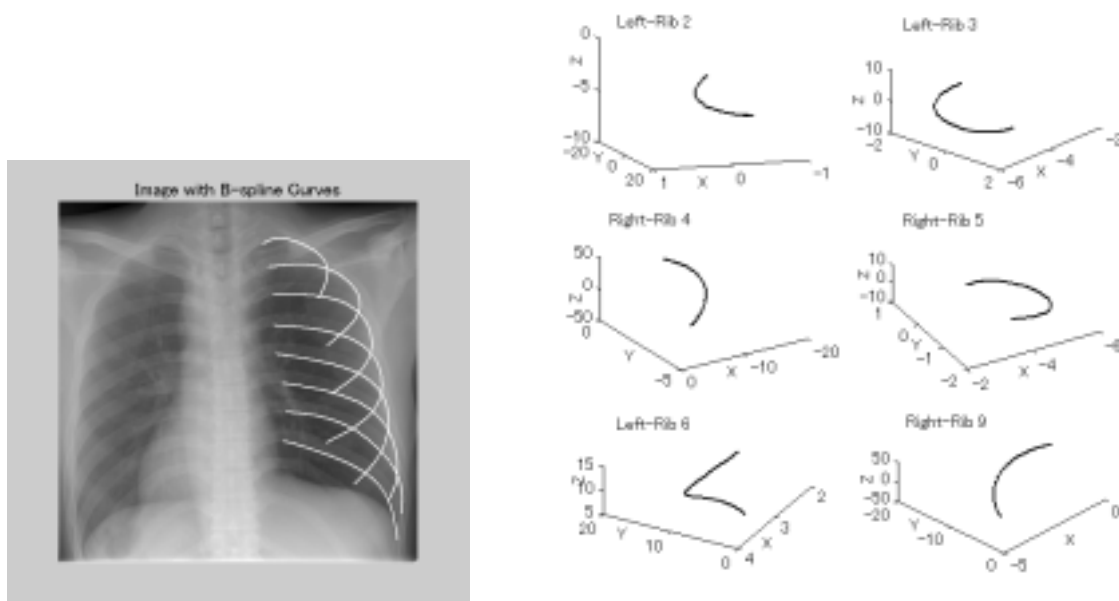(b) The curves of rib 2 in successive images.

Fig. 9 X-ray image with B-spline curves.   **Fig.10** Recovered 3D shapes of some ribs.

Table 2   Average error for the curve detection.

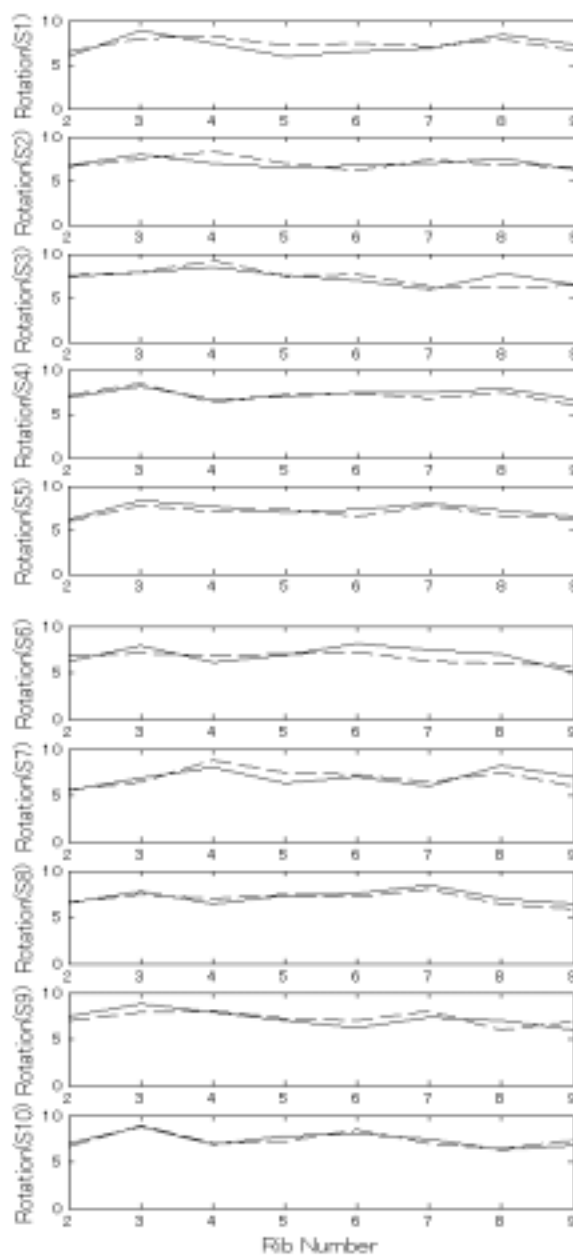|	Max-mean square errors (mm)	Average-mean square errors (mm)
Left ribs	0.21	0.15
Right ribs	0.22	0. 16
Average	0.215	0.155

5. Conclusions

A new method for detecting the 3D shape and motion of the rib is described in this paper. First, the set of control points for each curve (rib) is being extracted from the different images during breathing. Because our method uses only the control points instead of all points of a curve, data amount and computational times will be drastically reduced. Even through more than 60 points are included in a curve, only four control points for each curve are needed for computation. Furthermore, the accuracy of matching of a rib in multiple images is improved. Next, the 3D motion and 3D control points of each curve are estimated based on the factor decomposition method. Then the 3D shape of each rib has been reformed from these 3D control points. The average motion of the ribs has been determined.
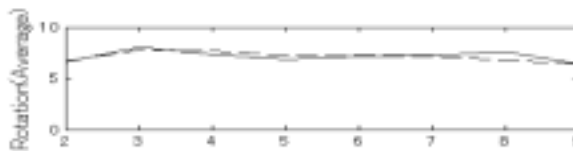
This method does not use a three-dimensional CT image but the 2D X-ray images. As for the patient, it is desired to investigate the breathing by standing up and it is not essential to put him on the bed. It is an advantage to investigate the breathing. This approach can be applied to examine the chest expansion for inspecting the pleural diseases such as chronic obstructive pulmonary disease (COPD), tuberculosis, ankylosing spondylitis, and adult respiratory distress syndrome and so on. It is also possible to analyze the modeling of the respiratory system. Our next work is to improve the precision of the motion and the shape of a rib with the more control points for each higher order spline curves. And we intend to reconstruct the whole shape of the rib cage based on the multi-object factorization approach under a perspective projection model. Moreover, we would like to investigate the breathing rate of abnormal people for comparing with these results.

Acknowledgement

(a)　Rotation angles of each subject

(b)　Average rotation angles.

Fig. 11 Rotation angle of ribs.

References

[1] Cala S.J., Kenyon C.M., Ferrignio G. et al.: Check wall and lung volume estimation by optical reference motion analysis, J. of Applied Physiology, Vol. 81, No. 6, pp. 2680-2689, 1996.

[2] De Groute A., Wantier M., Cheron G. et al.: Chest wall motion during tidal breathing, J. of Applied Physiology, Vol. 83(5), pp. 1531-1537, 1997.

[3] Jordanogulou J: Vector analysis of rib movement, Respiration Physiology, Vol. 10, pp. 109-120, 1970.

[4] Wilson T.A., Rehder K., Krayer S. et al.: Geometry and respiratory displacement of the human ribs, J. of Applied Physiology, Vol. 62(5), pp. 1872-1877, 1987.

[5] Park Y., Kitaoka H., Sato Y. et al. : 3D Analysis of the Respiratory Rib Motion for CT Images, IEICE DII, Vol. J83 -DII, No. 8, pp. 1618-1627, Aug. 2001.

[6] Ferrigno G, Carnevali P, Aliverti A et al.: Three-dimensional Optical Analysis of Chest Wall Motion. J Appl Physiol Vol. 77, No.3, pp. 1224-1231, 1994.

[7] Tomasi C. and Kanade T.: Shape and motion from image streams under orthography: A factorization method, Int. J. Computer Vision, 9(2), pp. 137-154, 1992.

[8] Bhuiyan M. A., Sein M. M. and Hama H.: On a Free Curve Maching Method—Algorithm for Finding the Control Points Bezier Curves and Similarity between Free Curves—, Proc. of the IASTED Int. Conf. Signal and Image Processing, SIP98, Lar Vegar, USA, pp. 473-477 , 1998.

[9] Sein M.M. and Hama H.: Recovering the 3D B-spline Control points of the Free Curve for Shape Reforming, IEICE translations on Information and Systems, Vol. E84-D, No. 8, pp. 983-989, Aug. 2001.